

High accuracy dual lens transmittance measurements

Jessica Cheung,¹ James L. Gardner,² Alan Migdall,³ Sergey Polyakov,^{3,*} and Michael Ware⁴

¹National Physical Laboratory, Teddington, UK, TW11 0LW

²National Measurement Institute, Lindfield 2070, Australia

³Optical Technology Division, National Institute of Standards and Technology, Gaithersburg, Maryland 20899-8441, USA
and Joint Quantum Institute, University of Maryland, College Park, Maryland 20742, USA

⁴Brigham Young University, Provo, Utah 84602, USA

*Corresponding author: spoly@nist.gov

Received 22 February 2007; revised 23 April 2007; accepted 28 April 2007;
posted 9 May 2007 (Doc. ID 80352); published 23 July 2007

We show how to determine the transmittance of short focal length lenses ($f \approx 19$ mm and $f \approx 25$ mm, in this case) with a combined uncertainty of 3 parts in 10^4 or better by measuring transmittances of lens pairs of a set of three or more lenses with the same nominal focal length. Uncertainties are minimized by optimizing the radiometric design of the setup and the measurement procedure. The technique is particularly useful in systems where the detector acceptance angle limits the beam geometry to relatively collimated beams. © 2007 Optical Society of America

OCIS codes: 120.7000, 120.3940, 220.3630.

1. Introduction

In metrology it is often necessary to measure the transmittance of optical components to a high level of accuracy and precision. A 'simple' transmittance measurement consists of using a spectrophotometer to measure the optical power of a beam with the optical element both in and out of the beam. The transmittance is then calculated as the ratio of these two measurements. Anderson *et al.* [1] discussed and Woolliams *et al.* [2] further developed a number of factors that must be considered when high accuracy transmittance measurements are required. Detector uniformity is important, because an optical element may displace the illuminated spot on the detector relative to the straight-through beam. It is also important to consider how the optical element modifies the beam geometry. For example, a lens alters the beam size and its divergence angle. Strongly focusing lenses cause the beam to diverge rapidly, so the acceptance angle limitations of the detector can become an issue. Other factors, such as antireflection coatings and their spectral variation may also need to be considered when determining transmittance.

Lenses, especially ones with short focal lengths, present a particularly challenging case for transmittance measurements because they significantly alter beam geometry. An example of where high accuracy transmittance measurements are required for short focal length lenses occurs in the calibration of high efficiency single-photon detectors used in quantum cryptography systems [3]. Related to this application is a recent high accuracy verification of a correlated-photon-based detection efficiency calibration method [4] that requires a high accuracy lens transmittance measurement. The active area of the photon-counting detectors used in this application is small (≈ 0.2 mm in diameter), so that short focal length lenses are required to collect the beam onto the device. Because the lens is in the calibration beam path, its transmittance must be accurately characterized so that the detector calibration can be corrected for signal lost due to less than unity transmittance.

Anderson *et al.* described a technique for measuring lens transmittance that provides for equal beam geometry at the detector with the lens in and out of the beam. Their technique uses two lenses with the same focal length f . The first measurement is made with one of the lenses a distance $2f$ from a light source and the detector distance $2f$ after the lens (position 1, Fig. 1), so that the detector is presented with a 1:1 (inverted) image of the source. For the second mea-

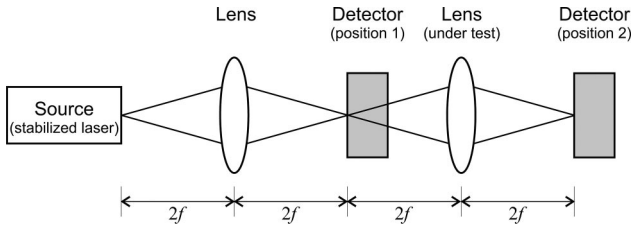


Fig. 1. Lens transmittance measurement technique developed at National Physical Laboratory (NPL) [2].

surement, the lens under test is placed a distance $4f$ from the first lens and the detector is moved $2f$ beyond the second lens (position 2), so that the detector is again presented with a 1:1 image of source. The detector is translated between positions 1 and 2 to measure the signal with and without the lens under test while maintaining the same beam geometry at both positions.

The technique depicted in Fig. 1 cannot be used in situations where the lens focal length becomes too short however, as there may not be enough physical space to implement the setup. In addition, the divergence of the beam can exceed the angular acceptance of the trap configuration detectors [5] that are often required for high accuracy measurements of this type. (Trap detectors are preferred over individual silicon photodiodes because of their low reflectance, excellent spatial uniformity, and low sensitivity to incidence angle, although they do have a limited angular acceptance range.) A different technique is therefore required to address the challenges posed by strongly focusing lenses.

In this article, we describe a ‘dual lens’ technique developed at the National Institute of Standards and Technology (NIST) to measure the transmittance of short focal length lenses. We illustrate its use by determining the transmittance of two different sets of lenses to a relative uncertainty of 0.1% or less (coverage factor $k = 1$). The technique is also appropriate for lenses with longer focal lengths.

2. Measurement Technique

This technique determines the transmittance of each lens of a set of three or more lenses, all with the same focal length. Pairs of lenses are mounted on a movable stage (separated by $\approx 2f$) so that the lens pair can be moved in and out of the beam (see Fig. 2). The source beam is collimated and the spacing of the lens pair is adjusted so that the beam at the detector is the same size with the lens pair in and out of the beam. This ensures that the beam geometry at the detector

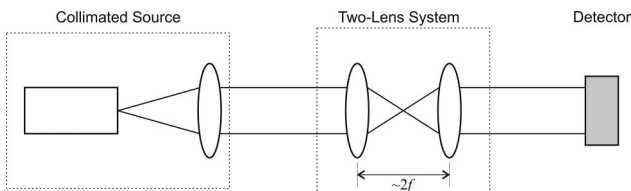


Fig. 2. Schematics of dual lens transmittance measurement.

is nominally the same with the lenses in and out, and that beam divergence is minimized at the detector. By comparing the signal with the lens pair in and out of the beam, the combined transmittance of the pair is measured. The process is then repeated for each possible pair combination of lenses in the set.

The pair transmittances measured in this setup are denoted as

$$m_{ij} = t_i t_j \quad (1 \leq i < j \leq N), \quad (1)$$

where N is the number of lenses in the measurement set, t_i and t_j are the individual lens transmittances, m_{ij} is their combined transmittance, and it is assumed that the lens order does not affect the lens pair transmittance. There are $C = N(N - 1)/2$ possible combinations of two lenses. For example, for three lenses ($N = 3$) there are three possible combinations ($C = 3$) and the equations specified by Eq. (1) are

$$m_{12} = t_1 t_2, \quad m_{13} = t_1 t_3, \quad m_{23} = t_2 t_3. \quad (2)$$

This is a set of nonlinear equations, which can readily be inverted to find the individual transmittances:

$$\begin{aligned} t_1 &= \sqrt{m_{12} m_{13} / m_{23}} \\ t_2 &= \sqrt{m_{12} m_{23} / m_{13}} \\ t_3 &= \sqrt{m_{13} m_{23} / m_{12}}. \end{aligned} \quad (3)$$

The values of m_{ij} are measured repeatedly so that each measurement has a mean value \bar{m}_{ij} and an associated standard deviation of the mean $\sigma_{m_{ij}}$. Henceforth we use m_{ij} to refer to this mean value. The individual transmittances are calculated using the mean values m_{ij} in Eq. (3), and the statistical uncertainties are determined using standard uncertainty propagation (assuming random noise dominates the measurement):

$$\sigma_{t_i} = \frac{1}{2} \sqrt{\left(\frac{\sigma_{m_{12}}}{m_{12}}\right)^2 + \left(\frac{\sigma_{m_{13}}}{m_{13}}\right)^2 + \left(\frac{\sigma_{m_{23}}}{m_{23}}\right)^2}. \quad (4)$$

To generalize this result to also include cases when more than 3 lenses are used, we rewrite equation set 1 as

$$\mathbf{m} = \mathbf{A} \mathbf{t}, \quad (5)$$

where

$$\mathbf{m} = \begin{bmatrix} \log(m_{12}) \\ \log(m_{13}) \\ \dots \\ \log(m_{1N}) \\ \log(m_{23}) \\ \dots \\ \log(m_{(N-1)N}) \end{bmatrix}, \quad \mathbf{A} = \begin{bmatrix} 1 & 1 & 0 & \dots & 0 & 0 \\ 1 & 0 & 1 & \dots & 0 & 0 \\ \dots & \dots & \dots & \dots & \dots & \dots \\ 1 & 0 & 0 & \dots & 0 & 1 \\ 0 & 1 & 1 & \dots & 0 & 0 \\ \dots & \dots & \dots & \dots & \dots & \dots \\ 0 & 0 & 0 & \dots & 1 & 1 \end{bmatrix},$$

$$\mathbf{t} = \begin{bmatrix} \log(t_1) \\ \dots \\ \log(t_N) \end{bmatrix}. \quad (6)$$

Here \mathbf{t} is a vector of dimension N , \mathbf{m} is a vector of dimension C (the number of possible lens combinations), and \mathbf{A} is a matrix of dimension $C \times N$. The matrix \mathbf{A} has two nonzero elements per row and $N - 1$ nonzero elements per column (all nonzero elements are equal to one). Because the measurements m_{ij} have nonzero uncertainty Eq. (5) will generally have no solution for $N > 3$ (i.e., the system is overdetermined for $N > 3$), but in these cases we can find a \mathbf{t}_0 that minimizes the norm $\|\mathbf{A}\mathbf{t}_0 - \mathbf{m}\|^2$. The value of \mathbf{t}_0 is our best estimate of the true value of \mathbf{t} given the overdetermined data set. The best estimate \mathbf{t}_0 always exists and can be found from

$$\mathbf{t}_0 = \mathbf{A}^+ \mathbf{m}, \quad (7)$$

where \mathbf{A}^+ is the Moore-Penrose generalized inverse matrix. In most cases, \mathbf{A}^+ can be constructed using $\mathbf{A}^+ = (\mathbf{A}^T \mathbf{A})^{-1} \mathbf{A}^T$ where T indicates the conjugate transpose. This method for finding the Moore-Penrose generalized inverse always works for the matrix \mathbf{A} defined in Eq. (6) as it can be shown by direct multiplication that $\mathbf{A}^T \mathbf{A} = \mathbf{1} + \mathbf{I}(N - 2)$, where $\mathbf{1}$ is a $N \times N$ matrix with all elements equal to 1 and \mathbf{I} is the identity matrix. Thus the rank of $\mathbf{A}^T \mathbf{A}$ is N and its inverse always exists. (In general, there are some rather exotic matrices where the inverse $(\mathbf{A}^T \mathbf{A})^{-1}$ does not exist, but that situation does not apply to the measurement system here and is thus beyond the scope of this paper [6,7].) For more details on the Moore-Penrose inverse, see the Appendix. Minimizing the norm $\|\mathbf{A}\mathbf{t}_0 - \mathbf{m}\|^2$ using Eq. (7), we obtain the following expression for the individual components of \mathbf{t}_0 :

$$t_n = \left(\frac{\prod_{i=n \text{ or } j=n} m_{ij}}{\left(\prod_{i \neq n \text{ and } j \neq n} m_{ij} \right)^{1/(N-2)}} \right)^{1/(N-1)}, \quad (8)$$

where n indicates the lens whose transmittance is being calculated and the constraints on i and j in the product limits are the same as in Eq. (1). The numerator of Eq. (8) contains the product of all measurements that include lens n , and the denominator contains a product of all the measurements that do not include lens n . Note that Eq. (8) reduces to Eq. (3) when $N = 3$. The relative uncertainties of the individual transmittances are calculated from

$$\frac{\sigma_{t_n}}{t_n} = \frac{1}{N-1} \sqrt{\sum_{i=n \text{ or } j=n} \left(\frac{\sigma_{m_{ij}}}{\bar{m}_{ij}} \right)^2 + \sum_{i \neq n \text{ and } j \neq n} \left(\frac{1}{N-2} \frac{\sigma_{m_{ij}}}{\bar{m}_{ij}} \right)^2} \quad (9)$$

using the mean values, and the relative uncertainty of the combined transmittances. (Again, random effects are assumed to dominate the measurement as in Eq. (4).)

After the set of transmittances is calculated using Eq. (8), and its uncertainty is estimated using Eq. (9), it is important to independently verify that the sta-

tistical variations of the components of the residual vector $\mathbf{A}\mathbf{t}_0 - \mathbf{m}$ are consistent with Eq. (9). This provides a check for possible systematic uncertainties and cross-correlations between the measurements. When the values of calculated lens transmittance t_0 are all similar, and the uncertainties σ_m are likewise comparable, we can approximate the uncertainty of a given transmittance by

$$\frac{\sigma_{t_n}}{t_n} \approx \left\langle \frac{\sigma_t}{t} \right\rangle \approx \sqrt{\frac{\|\mathbf{A}\mathbf{t}_0 - \mathbf{m}\|^2}{2(N-1)\langle m \rangle^2}}, \quad (10)$$

where $\langle \dots \rangle$ indicates a mean of all vector components. In our experiment, we estimate the uncertainty using both Eq. (9) and Eq. (10) and find that the values are consistent.

3. Choosing the Number of Lenses

In many situations the goal is to measure the transmittance of just a single lens. In this case, it is necessary to determine whether it is best to measure the transmittance with the minimum number of three lenses or with a larger overdetermined set. For convenience in writing, we will refer to the $N = 3$ case as the “just-determined” approach and the $N > 3$ as the “overdetermined” approach. To simplify our analysis of this question, we assume that $\sigma_{t_i} \approx \sigma_t$, $t_i \approx t$, and $m_{ij} \approx m$ for all values of i and j . This allows us to omit the notation $\langle \dots \rangle$ in Eq. (10). For a set of N lenses, there are $N(N - 1)/2$ possible lens combinations, of which $N - 1$ will contain the lens whose transmittance is of interest. If we assume that $\sigma_{m_{ij}} \approx \sigma_m$, then Eq. (9) reduces to

$$\frac{\sigma_t}{t} = \frac{\sigma_m}{m} \sqrt{\frac{2N-3}{2(N-1)(N-2)}}. \quad (11)$$

Thus, for a set of 4 lenses (the overdetermined approach), the uncertainty would be $\sqrt{15}\sigma_m/6m$, while for a set of 3 lenses (the just-determined approach), the uncertainty would be greater: $\sqrt{27}\sigma_m/6m$. However, there are twice as many lens-pairs in a set of four lenses (six pairs) as there are in a set of three lenses (three pairs). Thus, given a fixed total measurement time, we could double the time spent on each individual lens pair measurement for a set of three compared to a set of four. Assuming that the uncertainty is due to random processes, the measurement uncertainties decrease with measurement time as $1/\sqrt{\tau_{meas}}$. Additional time spent measuring the combinations with the 4th lens could instead be used to measure a smaller set of three lenses to a better uncertainty. If for example we are interested in the transmittance of lens 1, we see that $\sigma_{m_{ij}}$ with $i \neq 1$ contributes to Eq. (9) with lower weights than $\sigma_{m_{1j}}$ with $1 < j \leq N$. Thus, we could optimize the total measurement time by spending more time measuring m_{1j} , rather than m_{ij} , $i, j \neq 1$. We define Δ as the uncertainty ratio:

$$\Delta = \frac{\sigma_{m_{ij}}}{\sigma_{m_{ij}}} = \frac{\sigma_{m_{ij}}}{\sigma_m}, \quad (12)$$

with $\sigma_{m_{ij}} = \sigma_m$. Eq. (12) gives us a parameter that can be adjusted to minimize the final uncertainty with respect to the total measurement time. This is achieved by reducing the time spent measuring pairs that do not contain the lens of interest to τ_{meas}/Δ^2 . As before, we assume that all values of m and t are approximately equal. Equation (9) then becomes:

$$\left. \frac{\sigma_t}{t} \right|_{\text{overdetermined}} = \frac{\sigma_m}{m} \sqrt{\frac{2(N-2) + \Delta^2}{2(N-1)(N-2)}}. \quad (13)$$

The time of measurement of the entire lens set is

$$\tau_{tot} = (N-1) \left(1 + \frac{N-2}{2\Delta^2} \right) \tau_{meas}, \quad (14)$$

reflecting the fact that $(N-1)$ measurements on lens-pairs containing the lens of interest take τ_{meas} time each, while the rest require reduced time. We could have spent τ_{tot} differently, to measure the lens pairs of a minimal lens set of three. This would improve the uncertainty of the transmittance of the one lens of interest:

$$\left. \frac{\sigma_t}{t} \right|_{\text{just-determined}} = \frac{\sigma_m}{m} \sqrt{\frac{9\tau_{meas}}{4\tau_{tot}}}. \quad (15)$$

To compare the uncertainties of the overdetermined and 3-lens (just-determined) methods, consider the function

$$\Theta(\Delta, N) = \left(\left. \frac{\sigma_t}{t} \right|_{\text{overdetermined}} \right)^2 / \left(\left. \frac{\sigma_t}{t} \right|_{3 \text{ lens}} \right)^2. \quad (16)$$

If $\Theta(\Delta, N) < 1$, the overdetermined method yields lower uncertainty. Substituting Eqs. (13) and (15) in Eq. (16) we see that $\Theta(1, N) > 1$ for $N > 3$, showing that if time intervals are equal for all lens-pairs the three-lens method is better. We explored whether the overdetermined method could be improved by establishing an optimal Δ , that minimized Θ . We find the optimal Δ by differentiating Eq. (16):

$$\Delta_{\text{optimum}} = \frac{\sqrt{5(N-2)}}{2} > 1. \quad (17)$$

This yields $\Theta_{\text{optimum}} = 13/15$, which somewhat surprisingly does not depend on N . The fact that $\Theta_{\text{optimum}} < 1$ shows that after optimization the uncertainty improvement of the overdetermined lens method is $\sqrt{13/15}$, (or $\approx 7\%$) relative to the 3-lens method. The optimal time to spend measuring lens pairs containing the lens of interest should be

$5(N-2)/4$ larger than the time spent measuring the other lens-pairs.

In summary, we can say that when one wants the transmittance of only one lens, time should be spent improving the measurement uncertainty on the lens-pairs made from the minimal set of 3 lenses. When the lens-pair measurement uncertainty for this minimal 3-lens set can no longer be improved with longer measurement times, then more lenses should be added to the measurement procedure to improve the transmittance determination of the one lens of interest, in accordance with Eq. (11). While an advantage can be achieved by adjusting the time spent on lens pairs containing the lens of interest versus the other pairs, the 7% improvement may not be worth the effort. The matrix method is designed to efficiently determine the transmittances of all the lenses in the overdetermined set by minimizing all the uncertainties at once. Thus it is not surprising that it is not the best way to determine the transmittance of a single lens.

4. Experimental Details

We implemented the transmittance measurement setup (Fig. 3) and measured two sets of lenses using this technique. Both sets consisted of four achromatic doublet lenses that were antireflection (AR) coated on both sides for the wavelength range 650 nm to 1050 nm. One lens set had a focal length of $f = 19$ mm, and the other lens set had $f = 25$ mm. These lenses were to be used in a system for measuring the detection efficiency of single-photon detectors [8,9].

A. Laser Source

Our laser source was a power-stabilized cw Ti:sapphire laser tuned to 702.2 nm. To improve the spatial mode quality of the beam, we coupled the laser into a single-mode fiber and then collimated the output from the fiber into a beam ≈ 4 mm in diameter. A portion of the beam was split off with a wedged beam splitter and sent to a monitor detector to allow for correction of any residual fluctuations in laser power. To minimize effects due to the variations of the beam polarization out of the fiber, the beam splitter was oriented near normal incidence to the input beam. The monitor detector and the main-signal detector were read simultaneously. By taking a ratio of the two measurements, we were able to correct for residual fluctuations in the laser power. Figure 4 shows the ratio of the signal from both detectors measuring the laser

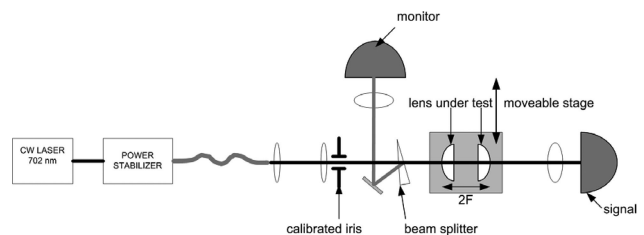


Fig. 3. Setup of dual lens transmittance measurement.

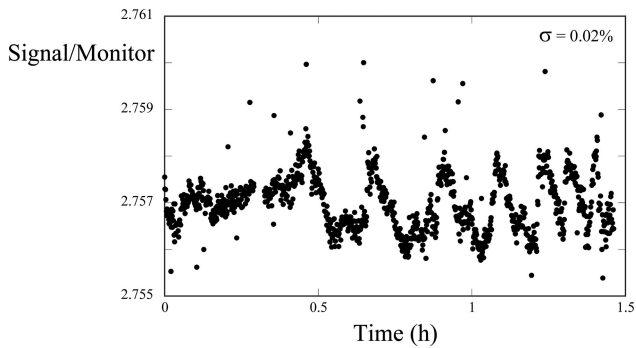


Fig. 4. Ratio of the signal and monitor trap detector outputs (with readings taken simultaneously).

beam over a period of ≈ 1.5 h. In addition to short time noise, there are clearly some periodic variations remaining in the ratio on time scales of 5 to 13 min. The uncertainties resulting from these short- and long-time variations are presented in the next section. The overall relative standard deviation of the ratio data over this period is 0.02% which is ≈ 13 times more stable than the signal from either individual trap detector.

B. Trap Detectors

Reflectance trap detectors were used for both the signal and monitor detectors. These trap detectors are constructed with three silicon photodiodes arranged so reflectance loss from each silicon photodiode is captured by subsequent photodiodes. This arrangement provides the excellent detector spatial response uniformity needed to achieve the high level of accuracy required for our particular application [5]. In addition, the configuration of these traps is such that polarization sensitivity is minimized. Typical net reflectance from a trap detector was less than 0.5% at the wavelength of interest (702.2 nm) compared with 30% for a single photodiode element [5]. The electronic signals from the trap detectors were read using current-to-voltage converters and digital multi-meters.

C. Beam Size

Transmittance measurements were carried out using several different beam sizes for one pair of lenses to test the sensitivity of the measurements to beam size. A calibrated iris was used to adjust the beam diameter. The lenses under test are small (12 mm diameter) and have highly curved surfaces, so it was expected that a small beam diameter would be more sensitive to its positioning on each lens. This was seen empirically by comparing measurements made with 2 mm and 4 mm beam diameters. The 4 mm beam yielded better reproducibility by a factor of 2 and was closer to the beam size used in the application that created the need for these lens measurements in the first place, so the 4 mm diameter was used for our measurements here.

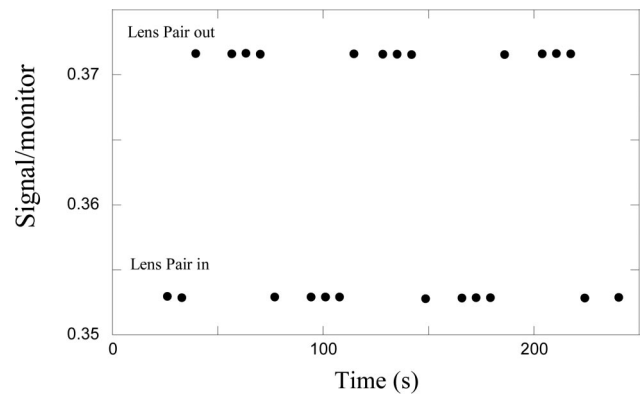


Fig. 5. Typical transmittance data for one run with a lens pair alternately in and out of the beam. Six such graphs are produced for the 6 lens pair combinations constituting one set of data.

D. Lens Alignment

The lenses were mounted in a pair of XY positioning lens holders attached to a single sliding translation stage that allowed easy and reproducible positioning of the lens-pair in and out of the beam. Beam pointing uncertainties were minimized by placing an alignment iris in front of the signal detector and adjusting the transverse positions of the two lenses so that the beam was incident on the same spot of the detector entrance with the lens system in and out. (Usually only minimal adjustments were necessary since the centers of the XY mounts were prealigned to the laser beam before inserting the lenses.) The alignment iris was opened for the measurement.

Once the lenses were aligned, a sequence of four readings was taken with the lens-pair in and then four readings with the lens-pair out. This was repeated 3 or 4 times for each lens-pair, constituting one run (see Fig. 5). One of the lenses would then be removed and replaced with another lens and the XY position of the new lens adjusted to re-center the beam on the detector. For four lenses, six pair combinations were possible—this constituted one data set. The whole procedure was then repeated several times.

E. Results

The 'in' and 'out' measurements were averaged and then ratioed to get an overall transmittance for each lens-pair and a relative standard deviation determined from the deviations of the 'in' and 'out' measurements. The other 5 lens-pair combinations of that data set were measured and analyzed similarly. Equation (8) was used to extract the transmittance for each individual lens. This procedure was repeated for several distinct data sets and a mean and uncertainty of the mean was determined for each lens. These uncertainties were compared against the uncertainties determined from the individual 'in' and 'out' measurements. Figure 6 shows the individual and average transmittance values for each lens and for each data set for the just-determined and over-determined analyses. In the just-determined case, each

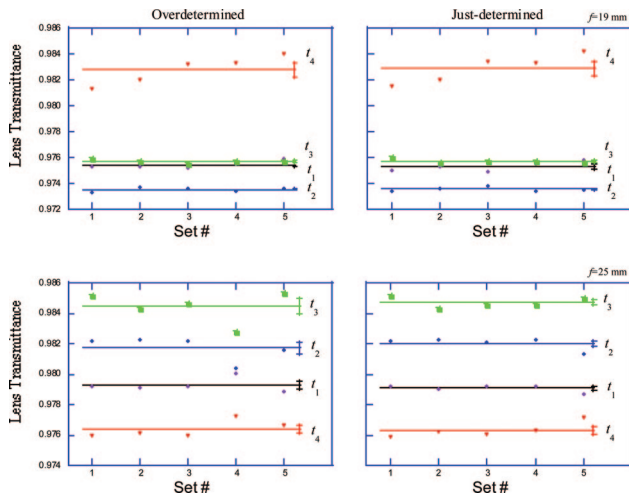


Fig. 6. (Color online) Transmittances (points) of four lenses with $f = 19$ mm (top) and four lenses with $f = 25$ mm (bottom) obtained using the overdetermined method (left) and the just-determined method (right). The averages (lines) over 5 sets are shown for each lens with uncertainties determined from the standard deviations of the 5 data sets for each lens type.

transmittance is calculated with Eq. (3) (using the three lens-pairs that include a given lens), and the uncertainties are calculated with Eq. (4). In the overdetermined case, the transmittances are calculated with Eq. (7) (which uses all six lens-pair measurements together), and the uncertainties are calculated with Eq. (9). The average over the data sets for each lens is also shown along with the uncertainties of those averages. Figure 7 shows that the results of the two analyses agree to within the uncertainties of the comparison. Both sets of lenses show transmittance values distributed with a standard deviation of $\approx 0.25\%$, although one of the eight lenses, the t_4 19 mm lens had a spread higher than the others and the measurements of the lens pair combinations containing this lens had a standard deviation more than 4 times the standard deviation of those not containing this lens. We note that although the nominal focal length of this one lens matched the 19 mm of the other lenses, its construction was different with a different thickness and surface curvatures. These differences may have contributed to the larger spread

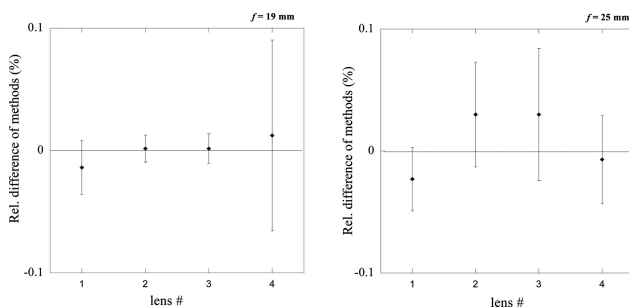


Fig. 7. Comparison of the transmittance results for the 19 mm and 25 mm lenses obtained using the just- and overdetermined methods.

perhaps due to additional alignment uncertainties (the lens pair separation was kept constant for all the measurements, so the resulting beam size would vary slightly at the detector), or the drift may have been due to changes in the lens itself. This situation suggests the importance of uniformity of construction in the lens set to be measured. Overall however, we do see that the two analysis methods agree on the transmittance result for each measurement set and this one lens does not appear to impact the other lens transmittances through increased drift or uncertainties.

The uncertainties given in Fig. 7 are the combined uncertainties taking into account all the measured uncertainties. The transmittances of both the $f = 25$ mm and $f = 19$ mm lenses were determined with uncertainties of 0.02% to 0.03% ($k = 1$) as shown in Table 1 for the just-determined and overdetermined analyses respectively. The Type A uncertainties (random), were obtained empirically from the repeatability between lens data sets. This variation is due to optical alignment of the lenses in combination with the trap responsivity nonuniformity, laser stability, and reflectance variation of the lens coating as its alignment changes slightly as the lens is repositioned between measurements. We use the empirical values because they were repeatable, but we also include simple estimates for the individual components in Table 1 for comparison and completeness (even though these estimates are much less well-determined). The Type A uncertainties clearly dominate the Type B uncertainties (systematic) that were estimated at an overall level of $\approx 2\%$ of the Type A uncertainties. The laser/monitor stability is broken up into a short-term component obtained from the

Table 1. Average Uncertainty Budget ($k = 1$) Showing the Effect of Each Uncertainty Component on the Lens Transmittance

Uncertainty Type	Uncertainty (%)	
	Just-Determined	Over-Determined
Type A (random)		
Trap nonuniformity	0.009	0.006
Laser/monitor stability		
Noise (short term)	0.004	0.003
Drift (long term)	0.006	0.005
Lens angular reflectance	0.004	0.003
Total	0.01	0.01
Total (empirical)	0.02	0.03
Type B (systematic)		
Wavelength uncertainty (0.01 nm)	0.00029	0.00021
Digital voltmeter	0.00022	0.00016
Reflected beam collection	0.00008	0.00006
Total	0.0004	0.0003
Total uncertainty	0.02	0.03

short-term noise seen in Fig. 4 and a long-term component drift also evident in the figure. Because the time between a lens-pair in and out measurement was only ≈ 30 s and a series of several such measurements contributed to a each transmittance determination, the net effect of the drift on the final transmittance is only slight larger than that due to the short-term effect. The largest Type B uncertainty is the laser wavelength uncertainty (0.01 nm), which has a sensitivity of $\approx 10^{-3}$ /nm on the uncertainty of the final result. Uncertainty due to the linearity and accuracy of the digital voltmeter is also shown. An uncertainty due to interreflections between the lenses resulting in additional light entering the trap detector is extremely small due to the high curvature of the lenses and the small solid angle subtended by the trap detector. (Note: The dominance of Type A uncertainties in our measurements is consistent with the fact that the uncertainties given by Eq. (9) are comparable to the residuals given by Eq. (10) for overdetermined data sets and consistent with the total uncertainties given in Table 1.)

5. Conclusions

We have discussed a dual sample technique that has been demonstrated to measure transmittance of short focal length lenses with a combined uncertainty of 3 parts in 10^4 or better. The technique provides a collimated beam geometry thereby reducing problems associated with limited acceptance angles of the detector system. This in turn allows the use of trap detectors [5], which typically have an acceptance angle of 4° and much better spatial uniformity than standard individual silicon photodiodes. The procedure uses measurements of pairs of nominally identical lenses in different combinations and extracts the transmittance of each individual lens by applying a generalized inverse matrix.

We also presented guidelines on when to spend additional time measuring a minimal set of three lenses or to add more lenses to the procedure to minimize measurement uncertainties. When one is interested in determining the transmittance of only one lens, it is usually best to use the lens-pairs made from the minimal set of 3 lenses. If the desired uncertainty in the transmittance cannot be achieved with the set of 3 lenses (i.e., the lens-pair measurement uncertainties cannot be improved with longer measurement times), then the uncertainty of the single lens of interest can be improved by adding additional lenses. However, the gains in uncertainty are increasingly small and the increase in measurement time is increasingly large with each additional lens.

Appendix: Minimal Property of Moore–Penrose Generalized Inverse

For the convenience of the reader we have summarized the well known basic properties of the generalized matrix inverse [6,7]. The pseudoinverse matrix \mathbf{A}^+ is defined so as to satisfy

$$\mathbf{AA}^+ = \mathbf{P}_{R(\mathbf{A})}, \quad \mathbf{A}^+\mathbf{A} = \mathbf{P}_{R(\mathbf{A}^+)}, \quad (18)$$

where $\mathbf{P}_{R(\mathbf{A})}$ is an orthogonal projector on range of \mathbf{A} (i.e., the linear span of columns of \mathbf{A}). The orthogonal projector is defined as $\mathbf{P}_{R(\mathbf{A})}\mathbf{u} = \mathbf{u}$ if $\mathbf{u} \in R(\mathbf{A})$, and $\mathbf{P}_{R(\mathbf{A})}\mathbf{u} = \mathbf{0}$ if $\mathbf{u} \in R(\mathbf{A})^\perp$ where $R(\mathbf{A})^\perp$ is the range orthogonal to $R(\mathbf{A})$. Using this we can write

$$\begin{aligned} \mathbf{At} - \mathbf{m} &= \mathbf{At} - \mathbf{AA}^+\mathbf{m} + \mathbf{AA}^+\mathbf{m} - \mathbf{m} \\ &= (\mathbf{At} - \mathbf{AA}^+\mathbf{m}) + [-(\mathbf{I} - \mathbf{P}_{R(\mathbf{A})})\mathbf{m}], \end{aligned} \quad (19)$$

where \mathbf{I} is an identity matrix. Because $\mathbf{At} \in R(\mathbf{A})$, $\mathbf{AA}^+\mathbf{m} = \mathbf{P}_{R(\mathbf{A})}\mathbf{m} \in R(\mathbf{A})$ and $(\mathbf{I} - \mathbf{P}_{R(\mathbf{A})})\mathbf{m} = \mathbf{P}_{R(\mathbf{A})^\perp}\mathbf{m} \in R(\mathbf{A})^\perp$, the expression in the first parentheses is orthogonal to the one in the second parentheses, so the norm of Eq. (19) can be written simply as

$$\|\mathbf{At} - \mathbf{m}\|^2 = \|\mathbf{At} - \mathbf{AA}^+\mathbf{m}\|^2 + \|\mathbf{AA}^+\mathbf{m} - \mathbf{m}\|^2. \quad (20)$$

Note, that only the expression in the first parentheses of Eq. (20) depends on \mathbf{t} . We require $\mathbf{At} - \mathbf{AA}^+\mathbf{m} = \mathbf{0}$, so $\mathbf{t} = \mathbf{A}^+\mathbf{m}$ makes the first term in Eq. (20) zero and hence minimizes the norm.

The most common way to build a generalized inverse matrix is to start with the equation $\mathbf{m} = \mathbf{At}$ and multiply it by a conjugate from the left $\mathbf{A}^T\mathbf{m} = \mathbf{A}^T\mathbf{At}$. Now, if the inverse of $\mathbf{A}^T\mathbf{A}$ exists, one can write $\mathbf{t} = (\mathbf{A}^T\mathbf{A})^{-1}\mathbf{A}^T\mathbf{m} = \mathbf{A}^+\mathbf{m}$, so $\mathbf{A}^+ = (\mathbf{A}^T\mathbf{A})^{-1}\mathbf{A}^T$. To cross-check if this form of the matrix satisfies the definition given by Eq. (18), we can use a simple property of projectors, that $\mathbf{P}_{R(\mathbf{A})}\mathbf{A} = \mathbf{A}$. Indeed, $\mathbf{P}_{R(\mathbf{A})}\mathbf{A} = \mathbf{AA}^+\mathbf{A} = \mathbf{A}(\mathbf{A}^T\mathbf{A})^{-1}\mathbf{A}^T\mathbf{A} = \mathbf{A}$.

This work was supported in part by the Disruptive Technology Office (DTO)-Army Research Office (ARO) Multidisciplinary University Research Initiative (MURI) Center for Photonic Quantum Information Systems program, and the UK DTI (Department of Trade and Industry) National Measurement Directorate.

References

1. V. E. Anderson, N. P. Fox, and D. H. Nettleton, "Highly stable, monochromatic and tunable optical radiation source and its application to high accuracy spectrophotometry," *Appl. Opt.* **31**, 536–545 (1992).
2. E. R. Woolliams, D. F. Pollard, N. J. Harrison, E. Theocharous, and N. P. Fox, "New facility for the high accuracy measurement of lens transmission," *Metrologia* **37**, 603–605 (2000).
3. B. Munro, "Quantum information processing with light and its requirement for detectors," presented at the NIST Single Photon Detection workshop, Gaithersburg, Maryland, USA, 31 March–1 April 2003.
4. S. V. Polyakov and A. L. Migdall, "High accuracy verification of a correlated-photon-based method for determining photon-counting detection efficiency," *Opt. Express* **15**, 1390–1407 (2007).
5. N. P. Fox, "Trap detectors and their properties," *Metrologia* **28**, 197–202 (1991).

6. S. L. Campbell and C. D. Meyer, Jr., *Generalized Inverses of Linear Transformations* (Pitman Publishing Limited, 1979).
7. A. B. Israel and T. N. E. Greville, *Generalized Inverses: Theory and Applications* (Wiley, 1974).
8. J. Y. Cheung, P. J. Thomas, C. J. Chunnillall, J. R. M. Mountford, and N. P. Fox, "Measurement of quantum efficiency using the correlated photon technique," extended abstract, presented at the NEWRAD 2005, 9th International Conference on Developments and Applications in Optical Radiometry, WRC/PMOD, Davos, Switzerland, 17–19 October 2005.
9. M. Ware and A. Migdall, "Single photon detector characterization using correlated photons: the march from feasibility to metrology," *J. Mod. Opt.* **51**, 1549–1557 (2004).